



HAL
open science

Pressure overload is associated with right ventricular dyssynchrony in heart failure with reduced ejection fraction

Luca Monzo, Marek Tupy, Barry A Borlaug, Adrian Reichenbach, Ivana Jurcova, Jan Benes, Lenka Mlateckova, Jiri Ters, Josef Kautzner, Vojtech Melenovsky

► To cite this version:

Luca Monzo, Marek Tupy, Barry A Borlaug, Adrian Reichenbach, Ivana Jurcova, et al.. Pressure overload is associated with right ventricular dyssynchrony in heart failure with reduced ejection fraction. ESC Heart Failure, 2024, 10.1002/ehf2.14682 . hal-04426979

HAL Id: hal-04426979


<https://hal.univ-lorraine.fr/hal-04426979v1>

Submitted on 30 Jan 2024

HAL is a multi-disciplinary open access archive for the deposit and dissemination of scientific research documents, whether they are published or not. The documents may come from teaching and research institutions in France or abroad, or from public or private research centers.

L'archive ouverte pluridisciplinaire **HAL**, est destinée au dépôt et à la diffusion de documents scientifiques de niveau recherche, publiés ou non, émanant des établissements d'enseignement et de recherche français ou étrangers, des laboratoires publics ou privés.

Pressure overload is associated with right ventricular dyssynchrony in heart failure with reduced ejection fraction

Luca Monzo^{1,2} , Marek Tupy¹, Barry A. Borlaug³, Adrian Reichenbach¹, Ivana Jurcova¹, Jan Benes¹, Lenka Mlateckova¹, Jiri Ters¹, Josef Kautzner¹ and Vojtech Melenovsky^{1*}

¹Institute for Clinical and Experimental Medicine (IKEM), Prague, Czech Republic; ²Université de Lorraine INSERM, Centre, d'Investigations Cliniques Plurithématique, Nancy, France; and ³Cardiovascular Division, Mayo Clinic, Rochester, MN, USA

Abstract

Aims The determinants and relevance of right ventricular (RV) mechanical dyssynchrony in heart failure with reduced ejection fraction (HFrEF) are poorly understood. We hypothesized that increased afterload may adversely affect the synchrony of RV contraction.

Methods and results A total of 148 patients with HFrEF and 36 controls underwent echocardiography, right heart catheterization, and gated single-photon emission computed tomography to measure RV chamber volumes and mechanical dyssynchrony (phase standard deviation of systolic displacement timing). Exams were repeated after preload ($N = 135$) and afterload ($N = 15$) modulation. Patients with HFrEF showed higher RV dyssynchrony compared with controls ($40.6 \pm 17.5^\circ$ vs. $27.8 \pm 9.1^\circ$, $P < 0.001$). The magnitude of RV dyssynchrony in HFrEF correlated with larger RV and left ventricular (LV) volumes, lower RV ejection fraction (RVEF) and LV ejection fraction, reduced intrinsic contractility, increased heart rate, higher pulmonary artery (PA) load, and impaired RV–PA coupling (all $P \leq 0.01$). Low RVEF was the strongest predictor of RV dyssynchrony. Left bundle branch block (BBB) was associated with greater RV dyssynchrony than right BBB, regardless of QRS duration. RV afterload reduction by sildenafil improved RV dyssynchrony ($P = 0.004$), whereas preload change with passive leg raise had modest effect. Patients in the highest tertiles of RV dyssynchrony had an increased risk of adverse clinical events compared with those in the lower tertile [T2/T3 vs. T1: hazard ratio 1.98 (95% confidence interval 1.20–3.24), $P = 0.007$].

Conclusions RV dyssynchrony is associated with RV remodelling, dysfunction, adverse haemodynamics, and greater risk for adverse clinical events. RV dyssynchrony is mitigated by acute RV afterload reduction and could be a potential therapeutic target to improve RV performance in HFrEF.

Keywords Heart failure with reduced ejection fraction; Right ventricular dyssynchrony; Right ventricular failure; Pulmonary hypertension; SPECT

Received: 9 August 2023; Revised: 19 November 2023; Accepted: 27 December 2023

*Correspondence to: Vojtech Melenovsky, Department of Cardiology, Institute for Clinical and Experimental Medicine (IKEM), Prague 140 21, Czech Republic. Tel: +420-739528029; Fax: +420-261362986. Email: vojtech.melenovsky@ikem.cz

Introduction

Left ventricular (LV) mechanical dyssynchrony has been extensively studied in patients with heart failure and reduced ejection fraction (HFrEF) due to its detrimental impact on LV performance and its implications for clinical outcomes.¹ The mechanisms and the relevance of right ventricular (RV) mechanical dyssynchrony in HFrEF are not well understood.

Mechanical dyssynchrony is an independent predictor of clinical worsening in primary diseases affecting the right ventricle, such as pulmonary arterial hypertension (PAH) or arrhythmogenic right ventricular cardiomyopathy,^{2,3} but studies in HFrEF are scarce.^{4,5}

Evaluation of RV function and mechanical synchrony is most often performed by echocardiography, but advanced echo-based techniques such as three-dimensional (3D) tissue

Doppler imaging or speckle tracking require highly standardized post-processing and are limited by geometric features of the right ventricle, angle dependency, intraoperator and inter-operator variability, acoustic windows, and image quality.⁶ In contrast, nuclear techniques for RV imaging, such as equilibrium gated single-photon emission computed tomography (GSPECT), are less hampered by the complex geometry of the right ventricle, are less operator dependent, and provide strong signal-to-noise ratio with isotropic 3D spatial information, allowing accurate quantification of RV volumes and function compared with echocardiography.^{7,8} Automated phase analysis of GSPECT data has been suggested as a promising and reproducible option for the evaluation of RV dyssynchrony.^{9,10}

The aim of this study was to investigate the correlates of RV dyssynchrony along with its prognostic significance in patients with advanced HFrEF using combined invasive–noninvasive pressure–volume analyses with acute load modulation. We hypothesized that increased RV load may adversely affect synchrony of RV contraction and as such contributing to worse RV chamber performance and prognosis.

Methods

Patient population

This prospective study enrolled patients with chronic (>6 months) symptomatic HFrEF [LV ejection fraction (LVEF) ≤40%] electively hospitalized for consideration of advanced therapies at the Institute for Clinical and Experimental Medicine (IKEM) in Prague, Czech Republic, from June 2016 to December 2020. All patients were followed up at IKEM (in the outpatient clinic or by planned elective hospitalization) at intervals dictated by the severity of their medical condition. Clinical events occurrence was ascertained by querying the hospital electronic records system and the national death registry. Patients with acute ischaemia, uncontrolled cardiac arrhythmia, haemodynamic instability needing inotropes or mechanical circulatory support, reversible cardiac dysfunction, active malignancy, endocrine disease, pre-existing treatment with a phosphodiesterase-5 (PDE5) inhibitor, and chronic or acute infection were excluded. To eliminate the confounding effect of pacing on RV dyssynchrony, only patients with native ventricular conduction were studied. In patients with an implanted cardiac device [implantable cardioverter defibrillator (ICD)/cardiac resynchronization therapy (CRT)], we ensured that the ventricle was not paced at the time of basal electrocardiogram (ECG), GSPECT, and right heart catheterization (RHC). Patients admitted with hypervolaemia were enrolled upon achieving normovolaemia, as determined by clinical judgement following the use of intravenous diuretics.

The control group consisted of individuals without HF (no clinical signs and symptoms typical of HF, no history of HF or HF-related hospitalizations, and normal natriuretic peptide levels) scheduled to undergo diagnostic or therapeutic procedures, including patients with unexplained shortness of breath of non-cardiac origin (11%) or patients undergoing closure of patent foramen ovale (89%).

The protocol was approved by the local ethics committee on 8 June 2016 (G-16-06-28, No. 986/16), and it was not considered as a clinical trial. All patients provided their informed consent for the procedures and for participating in this research study.

Study protocol

After signing informed consent, HF patients underwent history review, physical examination, echocardiography, ECG, Kansas City Cardiomyopathy Questionnaire, blood sampling, GSPECT, and RHC, as part of clinical work-up or for research purposes.

For the RHC procedure, to ensure uniformity of the pressure transducer setting, with the patient in the supine position, the zero level was established at the mid-thoracic line as recommended.¹¹ During shallow respiration, a 10 s strip of ectopy-free, high-quality signal was used to record and annotate pressure waveforms (Mac-Lab, GE Healthcare, Chicago, IL). Using a 7 Fr balloon-tipped triple-lumen Swan-Ganz catheter (Braun Melsungen AG, Melsungen, Germany) inserted via the right internal jugular vein, invasive pressures were measured in the right atrium and right ventricle. Then the catheter was advanced to the pulmonary artery (PA), and its position was verified by identifying the signature pressure curves. Systolic (sPAP), diastolic (dPAP), and mean (mPAP) PA pressure, as well as the mean values of respiratory-averaged PA wedge pressure (PAWP), were measured as previously described.¹¹ Cardiac output (CO) was measured by thermodilution as the average of at least three measurements [five in patients with atrial fibrillation (AF)] with a variance of <10%.¹² In patients with AF, pressure waveforms were recorded during ectopy-free periods with the smallest R-R interval variability and averaged over several cardiac cycles.¹¹ The systemic blood pressure (SBP) was measured after 10 min of rest in the supine position using an automated oscillometric monitor.

After RHC, patients underwent ECG-gated 3D equilibrium ^{99m}Tc-labelled blood pool GSPECT. All patients received an injection of stannous pyrophosphate (Technescan PYP, Curium, The Netherlands), and 30 min later, erythrocytes were *in vivo* labelled by intravenous injection of 740 MBq ^{99m}Tc isotope. The heart chambers were imaged using a D-SPECT camera (Spectrum Dynamics, Israel) equipped with collimated, pixilated cadmium zinc telluride crystal detectors allowing rapid (7 min) data acquisition with high spatial resolution (mean ef-

fective dose ~ 5 mSv).¹³ Medications and conditions for examinations at both RHC and GSPECT were identical.

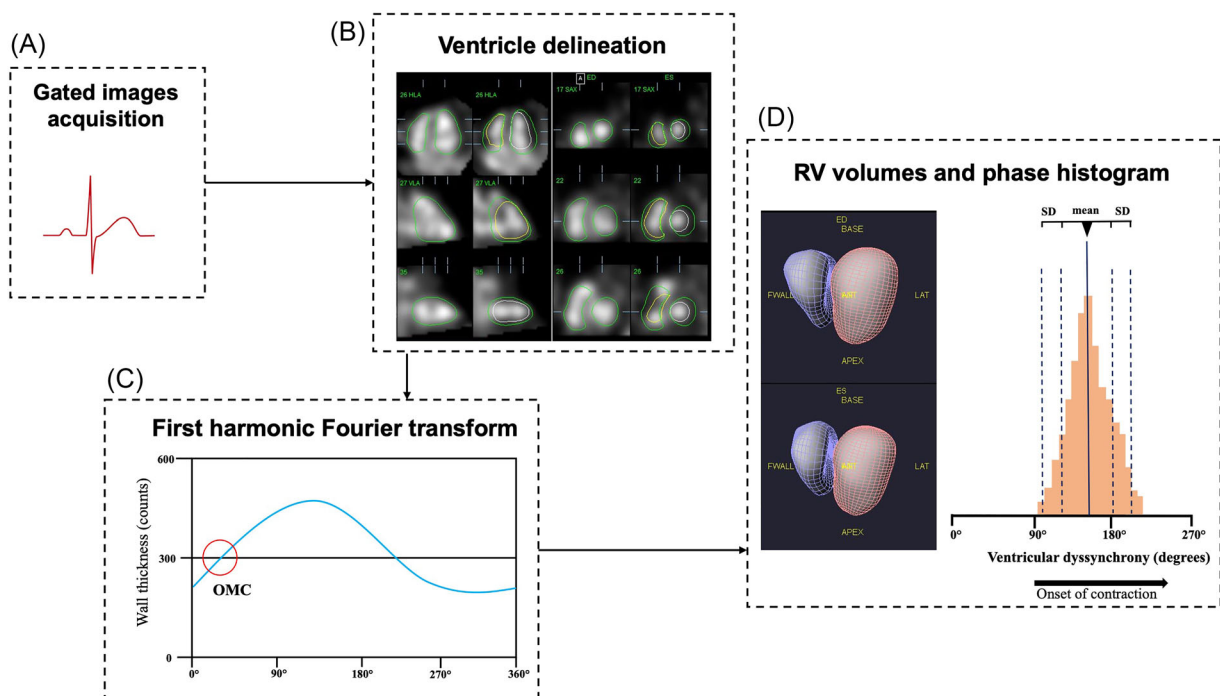
In a subgroup of HF patients, we explored the impact of afterload reduction ($n = 15$) and preload increase ($n = 135$) on RV dyssynchrony. Afterload reduction (achieved by administration of 20 mg intravenous sildenafil) was attempted in all euvolaemic subjects [right atrial (RA) pressure < 10 mmHg] with a significant pre-capillary component of pulmonary hypertension [i.e. pulmonary vascular resistance > 3 Wood units (WU) or transpulmonary gradient > 15 mmHg] and without systemic hypotension (SBP > 90 mmHg), as part of the standard protocol for pre-transplant evaluation in our centre.¹⁴ Haemodynamic assessment was performed before and 10 min after administering intravenous sildenafil, as part of the clinical evaluation protocol for HF patients. Patients who were administered sildenafil during RHC, underwent GSPECT imaging at least 35 h later (five times the elimination half-time of sildenafil), following which the sildenafil administration was repeated.

Preload increase was attempted in all patients unless technical or logistical issues occurred and was achieved by raising the legs of the patient by a 60° angle foam wedge for 7 min. Data acquisition for both GSPECT and RHC procedures started 30–60 s following the leg rise manoeuvre.

Haemodynamic and right ventricular pressure–volume analysis

The raw GSPECT data were post-processed by a single experienced nuclear physician (M.T.) using a semiautomatic commercially available plug-in software (QBS Cedars-Sinai, Los Angeles, CA) to obtain assessment of 3D volumes and systolic function in the time domain (*Figure 1* and Supporting Information, *Figure S1* and *Videos S1–S3*). Intraoperator reproducibility for GSPECT measures was assessed on 15 random subjects from the entire population. The Bland–Altman analysis showed a satisfying intraoperator reproducibility for both

Figure 1 Schematic illustration of the processing steps involved in the assessment of right ventricular (RV) dyssynchrony and volumes using gated myocardial perfusion single-photon emission computed tomography (SPECT) studies. After acquisition of electrocardiogram (ECG)-gated raw radionuclide angiocardiology (A), left and right ventricles were delineated by automatic processing on planar projections (B). For each temporal frame, a regional maximal count detection was performed. Consecutively, the first Fourier harmonic function was used to approximate the discrete sample points into a continuous wall-thickening curve (C). Based on the partial volume effect, this time–activity curve represents the thickening curve of this particular myocardial sample during a cardiac cycle. The point at which the continuous thickening curve intersects with the average count density of this voxel (horizontal line) is considered the onset of mechanical contraction (OMC) for this region (red circle). The software computes the OMC for all RV myocardial samples collected and then displays the composite result as a phase histogram. The surfaces resulting from ventricular delineation (Step B) are used to compute endocardial volumes at each interval of the gated data set and presented in a 3D reconstruction (D). The phase histogram was used to obtain the RV dyssynchrony indices, such as the phase mean and standard deviation (i.e. the standard deviation of the OMC phase distribution).



RV end-diastolic (mean bias 8.9 mL) and end-systolic (mean bias -4.3 mL) volumes (Supporting Information, *Figure S2*). GSPECT-derived ventricular volumes and RHC-derived pressures data were combined to calculate RV loading and contractility. Lumped RV afterload [PA elastance (E_{aPA})] was estimated as the sPAP divided by the stroke volume (derived from thermodilution CO). The choice to utilize sPAP instead of mPAP for E_{aPA} assessment stems from the observation that when pulmonary vascular impedance is elevated, sPAP provides a closer approximation of end-systolic pressure, whereas mPAP tends to underestimate it.^{15,16} RV contractility was estimated using the simplified formula for end-systolic elastance (E_{es}) calculated as the RV maximal pressure/end-systolic volume (derived from GSPECT).¹⁷ From these measurements, we derived ventricular–arterial coupling, calculated as $RV\ E_{es}/E_{aPA}$. PA compliance was calculated as the RHC-derived stroke volume/PA pulse pressure, and the pulmonary vascular resistance (PVR) was calculated as transpulmonary gradient (mPAP $-$ PAWP)/CO.¹⁸ RV diastolic compliance was determined by the ratio of end-diastolic pressure (EDP) to end-diastolic volume (EDV), a measurement that has been shown to agree with the more rigorous diastolic elastance coefficient β calculated from a curvilinear adjustment of end-systolic and EDP/EDV ratios.¹⁹ Pulmonary hypertension was defined as mPAP $>$ 20 mmHg.²⁰

Right ventricular dyssynchrony analysis

Phase analysis of GSPECT data was performed by a semiautomatic software (QBS Cedars-Sinai, Los Angeles, CA) as previously described.^{21,22} The program performed Fourier transformation on the 16-frame time–activity curve of each myocardial sample to derive the first harmonic function. The temporal onset of ventricular mechanical contraction during the cardiac cycle of each myocardial sample was considered to be the phase of the inflection point of the thickening curve on a horizontal line representing the average myocardial count over a cardiac cycle.²³ The onset of ventricular mechanical phase information from the RV myocardial samples collected was used to generate a phase distribution, which is displayed in histogram. Phase standard deviation [PSD, i.e. the standard deviation (SD) of the phase distributions during cardiac cycle in degrees] was used to express dyssynchrony as previously described (*Figure 1*).^{22,24} In unselected patients and control subjects, the repeatability of phase analysis approach is high and mainly attributable to automated generation of dyssynchrony parameters.^{22,25}

Data analysis

Data are shown as mean \pm SD or median and [25th–75th inter-quartile range (IQR)] for continuous variables (accord-

ing to distribution) and total count (n) with proportion (%) for categorical variables. One-way ANOVA and Kruskal–Wallis tests were used to compare continuous variables between groups depending on the normality of the distribution, and the χ^2 test was used for categorical variables. Normality was assessed using the Shapiro–Wilk test. Trend tests were performed by using the Cochran–Armitage or Cuzick’s trend test for categorical variables, and the Jonckheere–Terpstra test or linear regression for continuous variables, as appropriate. To assess the association of each variable with the severity of RV dyssynchrony (PSD), separate multiple logistic regression analyses were conducted. Variables not normally distributed had been log-transformed before the analysis. Pearson r or Spearman’s coefficient (for abnormally distributed variables) was calculated for correlations. Highly significant univariate variables (P value $<$ 0.001) were included in the multivariate model. Cox proportional hazard regression was used to analyse the factors associated with the adverse outcome, defined as combined endpoint of death, urgent transplantation, or left ventricular assist device (LVAD) implantation without heart transplantation, as done before.^{26–28} Kaplan–Meier curves with the log-rank statistics were used to illustrate the outcome. The effect of preload and afterload modulation on haemodynamic and GSPECT parameters was tested using paired t -test or the Wilcoxon signed-rank test as appropriate. A P value $<$ 0.05 was considered significant. All analyses were performed using JMP Pro 17.0 statistical software (SAS Institute, Inc., Cary, NC).

Results

Baseline characteristics: heart failure with reduced ejection fraction vs. controls

Patients with HFrEF ($n = 148$) were mostly middle-aged men with severe symptoms [77% in New York Heart Association (NYHA) Class III/IV] treated with optimized medical therapy (Supporting Information, *Table S1*). The median duration of HF was 3.6 [1.4; 7.5] years. As expected, patients with HFrEF displayed dilatation and impaired function of both ventricles compared with controls ($n = 36$), wider QRS duration, and higher natriuretic peptides. Nearly half (42%) of patients with HFrEF displayed RV dysfunction [RV ejection fraction (RVEF) \leq 35%]. The median time between RHC and GSPECT was 1 day (IQR, 0–1 day). At baseline, the majority of patients with HFrEF had combined post-capillary and pre-capillary pulmonary hypertension [mPAP 34.3 ± 10.8 mmHg, PAWP 22.8 ± 8.5 mmHg, PVR 2.9 (1.9; 4.2) WU], with low CO (3.8 ± 0.9 L/min) (Supporting Information, *Table S2*). A total of 128 patients (87%) with HFrEF had pulmonary hypertension, and 110 (74%) had PVR $>$ 2 WU.

Table 1 Baseline characteristics by RV dyssynchrony tertiles

	Tertile 1 (RV phase SD ≤ 30°) N = 49	Tertile 2 (RV phase SD 31–49°) N = 54	Tertile 3 (RV phase SD ≥ 50°) N = 45	P value ^a
Clinical characteristics				
Age (years)	55 ± 8	55 ± 10	52 ± 11	0.105
Male, n (%)	44 (90)	45 (83)	36 (80)	0.188
NYHA class, n (%): I–II; III–IV	10 (20); 39 (80)	14 (26); 40 (74)	10 (22); 35 (78)	0.822
Ischaemic HF aetiology, n (%)	29 (59)	22 (41)	14 (31)	0.006
Haemoglobin (mg/L)	136.9 ± 19.8	136.3 ± 16.5	137.6 ± 19.3	0.881
BNP (ng/L)	906 [390; 1796]	969 [524; 1930]	1,146 [665; 1835]	0.128
Echocardiography^b				
Mitral regurgitation, n (%): 0–2 grade; 3–4 grade	27 (56); 21 (44)	23 (43); 30 (57)	18 (41); 26 (59)	0.136
Tricuspid regurgitation, n (%): 0–2 grade; 3–4 grade	32 (65); 17 (35)	35 (66); 18 (34)	27 (63); 16 (37)	0.808
Electrocardiography				
Heart rate (b.p.m.)	77 ± 16	79 ± 13	85 ± 16	0.012
QRS morphology, n (%): LBBB; RBBB; normal; other alterations ^c	4 (8); 7 (14); 17 (35); 21 (43)	16 (30); 5 (9); 11 (20); 22 (41)	11 (24); 1 (2); 8 (18); 25 (56)	0.191
QRS duration (ms)	116.4 ± 25.2	123.3 ± 24.7	118.7 ± 24.4	0.639
Therapy				
ACE, ARB, or ARNI, n (%)	37 (76)	35 (65)	31 (69)	0.470
ACE, ARB, or ARNI ≥50% target dose, n (%)	17 (46)	17 (49)	15 (48)	0.835
MRA, n (%)	45 (92)	46 (85)	37 (82)	0.170
MRA ≥50% target dose, n (%)	40 (91)	44 (96)	33 (89)	0.819
Beta-blocker, n (%)	41 (84)	47 (87)	36 (80)	0.644
Beta-blocker ≥50% target dose, n (%)	16 (40)	12 (26)	13 (36)	0.684
Devices, n (%): ICD; CRT; none	40 (82); 3 (6); 6 (12)	40 (74); 7 (13); 7 (13)	31 (69); 2 (4); 12 (27)	0.117
Haemodynamic				
RA mean pressure (mmHg)	8.7 ± 6.0	9.9 ± 5.6	10.2 ± 5.8	0.222
RV systolic elastance (Ees) (mmHg/mL)	0.36 [0.24; 0.62]	0.32 [0.22; 0.47]	0.25 [0.21; 0.43]	0.010
RV diastolic compliance (mL/mmHg)	13.8 [9.9; 25.3]	12.6 [8.0; 17.4]	8.8 [6.3; 13.4]	<0.001
Cardiac output (L/min)	4.1 ± 0.8	3.6 ± 0.9	3.6 ± 1.0	0.007
Stroke volume (mL)	55.1 ± 14.1	47.2 ± 12.9	43.8 ± 15.3	<0.001
PA mean pressure (mmHg)	31.1 ± 12.1	35.2 ± 9.0	36.6 ± 10.5	0.014
PA wedge pressure (mmHg)	20.5 ± 9.4	23.3 ± 7.2	24.9 ± 8.1	0.012
PA compliance (mL/mmHg)	2.2 [1.7; 3.3]	1.7 [1.2; 2.4]	1.7 [1.2; 2.4]	0.010
PA elastance (E _{app}) (mmHg/mL)	0.91 [0.56; 1.22]	1.11 [0.80; 1.58]	1.27 [0.95; 1.76]	<0.001
PVR (WU)	2.3 [1.6; 3.1]	3.1 [2.4; 4.4]	3.1 [2.2; 4.7]	0.015
RV–PA coupling ratio	0.40 [0.26; 0.97]	0.28 [0.19; 0.41]	0.26 [0.14; 0.38]	<0.001
Systolic blood pressure (mmHg)	109.8 ± 14.6	109.9 ± 14.5	108.8 ± 19.9	0.765
Diastolic blood pressure (mmHg)	74.2 ± 8.5	76.4 ± 8.1	74.9 ± 13.2	0.719
GSPECT				
RV end-diastolic volume (mL)	256.9 ± 106.7	283.4 ± 90.9	287.9 ± 88.3	0.113
RV end-systolic volume (mL)	135.7 ± 82.6	180.1 ± 77.8	201.3 ± 81.7	<0.001

(Continues)

Table 1 (continued)

	Tertile 1 (RV phase SD $\leq 30^\circ$) N = 49	Tertile 2 (RV phase SD $31\text{--}49^\circ$) N = 54	Tertile 3 (RV phase SD $\geq 50^\circ$) N = 45	P value ^a
RV ejection fraction (%)	50.9 \pm 14.2	38.2 \pm 11.1	32.2 \pm 12.0	<0.001
LV end-diastolic volume (mL)	342.0 \pm 104.7	388.4 \pm 110.1	406.9 \pm 112.7	0.005
LV end-systolic volume (mL)	246.2 \pm 92.9	296.6 \pm 98.2	314.9 \pm 103.9	0.001
LV ejection fraction (%)	29.2 \pm 9.4	23.9 \pm 7.3	23.2 \pm 7.9	<0.001

ACE, angiotensin-converting enzyme; ARB, angiotensin receptor blocker; ARNI, angiotensin receptor–neprilysin inhibitor; BNP, brain natriuretic peptide; CRT, cardiac resynchronization therapy; GSPECT, gated single-photon emission computed tomography; ICD, implantable cardioverter defibrillator; LBBB, left bundle branch block; LV, left ventricular; MRA, mineralocorticoid receptor antagonist; NYHA, New York Heart Association; PA, pulmonary artery; PVR, pulmonary vascular resistance; RA, right atrial; RBBB, right bundle branch block; RV, right ventricular; SD, standard deviation; WU, Wood units.

^aP value for trend.
^bMitral regurgitation and tricuspid regurgitation were assessed semi-quantitatively and reported using a four-stage grading (i.e. 0 = none-trace, 1 = mild, 2 = moderate, and 3 = severe).

^cOther alterations include left anterior fascicular block, left posterior fascicular block, incomplete LBBB, and nonspecific intraventricular conduction delay.

Right ventricular dyssynchrony

Patients with HF_{rEF} showed higher degree of RV dyssynchrony compared with controls (Supporting Information, Table S2). Based on the distribution in HF patients, RV dyssynchrony tertiles were created with cut-offs $\leq 30^\circ$ ($N = 49$), $31\text{--}49^\circ$ ($N = 54$), and $\geq 50^\circ$ ($N = 45$). Patients with HF_{rEF} falling in the lowest tertile of RV synchrony had lower heart rate and higher prevalence of ischaemic HF aetiology compared with patients in the highest tertile. In haemodynamic examination, patients with lower degree of RV dyssynchrony showed more favourable afterload (lower E_{aPA}) and intracardiac pressures (lower PAWP), a better systolic function (higher CO and RVEF/LVEF and more preserved RV ventricular–arterial coupling ratio), and lower RV/LV volumes compared with higher tertiles (Table 1).

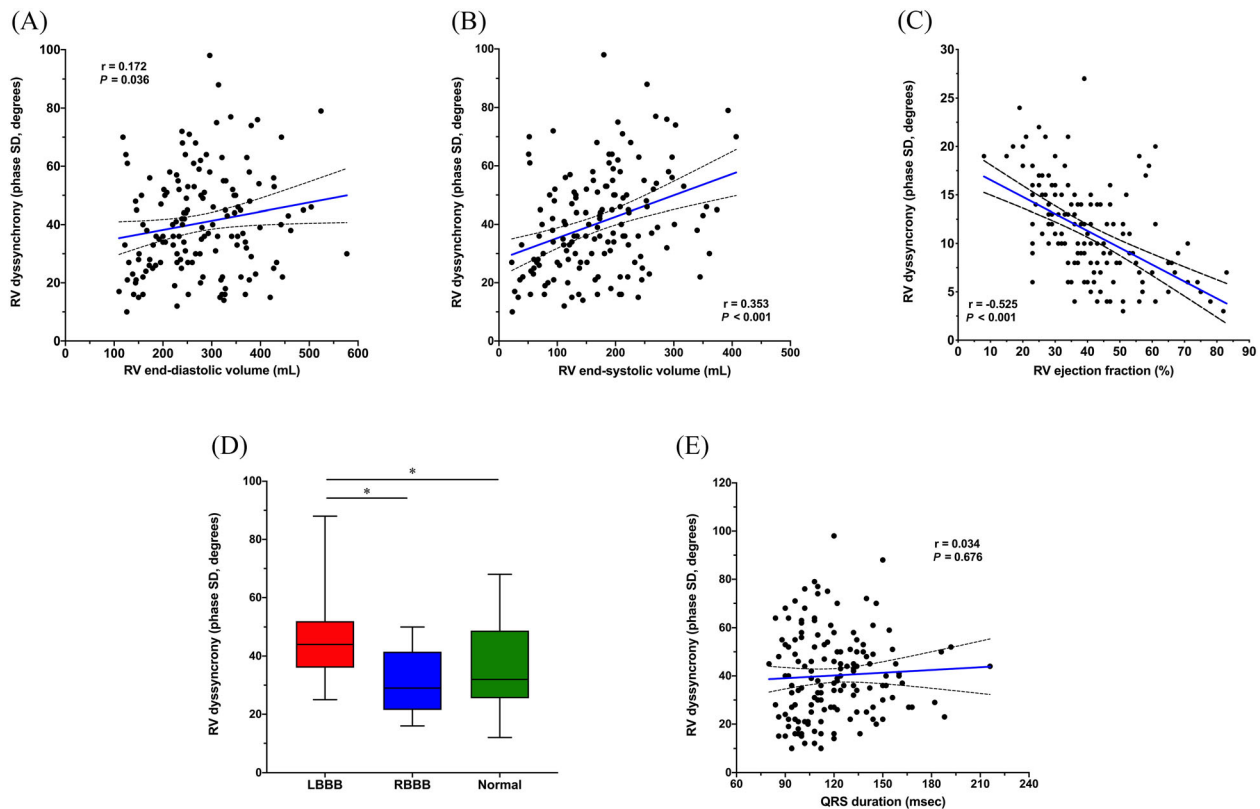
The degree of RV dyssynchrony was directly correlated with RV volumes (end-diastolic: $r = 0.172$, $P = 0.036$; end-systolic: $r = 0.353$, $P < 0.001$) and inversely correlated with RVEF ($r = -0.525$, $P < 0.001$) (Figure 2A–C and Table 2). From a haemodynamic perspective, increased RV afterload (expressed by the lumped RV afterload parameter PA elastance) and decreased RV end-systolic elastance were correlated with greater RV dyssynchrony (Supporting Information, Figure S3A,B). In addition, worse ventricular–arterial coupling ratio, larger LV volumes, and lower LVEF (Supporting Information, Figure S3C–F and Table 2), as well as higher PAWP and lower CO, were correlated with RV dyssynchrony. Patients with native left bundle branch block (LBBB) had more RV dyssynchrony than those with native right bundle branch block (RBBB) ($45.7 \pm 13.9^\circ$ vs. $30.9 \pm 11.1^\circ$, $P < 0.001$), regardless of QRS duration (Figure 2D,E). Those with non-ischaemic HF aetiology showed worse RV dyssynchrony ($44.3 \pm 17.8^\circ$ vs. $35.8 \pm 15.8^\circ$, $P = 0.003$), larger RV volumes (end-diastolic: 302 ± 98 vs. 243 ± 83 mL, $P < 0.001$; end-systolic: 199 ± 86 vs. 138 ± 69 mL, $P < 0.001$), and lower RVEF ($36 \pm 13\%$ vs. $46 \pm 15\%$, $P < 0.001$) compared with ischaemic patients (Supporting Information, Figure S4). No significant differences in terms of RV dyssynchrony were found among patients with and without AF ($37 \pm 19^\circ$ vs. $41 \pm 17^\circ$, $P = 0.414$). Among clinical parameters, a faster heart rate was correlated with a higher degree of RV dyssynchrony (Table 2).

In multivariable regression analysis, baseline low RVEF remained the only independent predictor of RV dyssynchrony. Excluding RVEF from the multivariate model, ventricular–arterial coupling and LVEF emerged as significant predictors of RV dyssynchrony (Table 2).

Preload and afterload modulation

The median time between RHC and GSPECT in this subgroup of patients was 2 days (IQR, 1–4 days). Compared with base-

Figure 2 Correlation between right ventricular (RV) dyssynchrony and (A) RV end-diastolic volume, (B) RV end-systolic volume, and (C) RV ejection fraction [all in heart failure with reduced ejection fraction (HFrEF) patients]. (D) RV dyssynchrony in HFrEF patients with left bundle branch block (LBBB), right bundle branch block (RBBB), and normal conduction. (E) Correlation between RV dyssynchrony and QRS duration in HFrEF patients. Asterisk stands for $P < 0.05$.



line, intravenous sildenafil ($N = 15$) decreased RA [-52 (-60 ; -37) %] and RV [RV EDP: -50 (-69 ; -25) %] pressure, RV afterload [$E_{a_{pA}}$ -43 (-54 ; -26) %], and PAWP [-20 (-43 ; 0) %] (Figure 3A) while increased CO [14 (2 ; 30) %] (all $P < 0.01$). It also reduced RV volumes [end-diastolic: -16 (-28 ; -8) %; end-systolic: -39 (-48 ; -16) %] and increased RVEF [$+23$ (20 ; 52) %] (Figure 3B) (all $P < 0.01$), without significantly affecting RV Ees [0.01 (-0.11 ; 0.12) mmHg/mL] (Supporting Information, Table S3). On the left side, sildenafil infusion significantly reduced systolic blood pressure [-6.1 (-11.6 ; -0.5) mmHg] and systemic vascular resistance [-376 (-564 ; -188) dyn/s/cm $^{-5}$]. RV dyssynchrony decreased following sildenafil administration [-15.0° (-22.0° ; 5.0°), $P = 0.004$] (Figure 3C).

Preload increase with passive leg raise ($N = 135$) significantly increased RA pressure [$+26$ (10 ; 46) %], RV EDP [27 (11 ; 56) %], RV afterload [$E_{a_{pA}}$ $+11$ (-3 ; 29) %], and PAWP [15 (3 ; 36) %] (all $P < 0.05$), without a relevant impact on CO [$+1$ (-9 ; 5) %]. A slight albeit significant increase was noted in RV volumes [end-diastolic: $+5$ (-4 ; 16) %; end-systolic: $+5$ (-8 ; 18) %], all $P < 0.05$, without significant changes in RVEF [0 (-12 ; 13) %] and RV Ees [-0.01 (-0.04 ; 0.02)

mmHg/mL] (Supporting Information, Table S3). Preload modulation had a modest influence on RV dyssynchrony in the overall population ($P = 0.080$) (Supporting Information, Table S3) but resulted in a significant RV dyssynchrony improvement in the subgroup of patients who underwent PDE5 inhibitors administration to test afterload reduction (Supporting Information, Figure S5). The effect of preload modulation was not significantly different between patients with and without AF [-1.9° (-11.7° ; 7.9°) vs. -2.7° (-5.9° ; 0.4°), $P = 0.373$].

Outcome

During a median follow-up of 206 days (IQR, 58–439 days), there were 83 composite events including 44 deaths, 33 assist device implantations, and 16 urgent cardiac transplantations. In univariable Cox regression analysis, the risk of composite outcome increased with higher RV dyssynchrony (Figure 4). In particular, patients in the highest tertiles of RV dyssynchrony (i.e. $>30^\circ$) had an increased risk of adverse clinical events compared with those in the lower tertile {T2/T3 vs.

Table 2 Variables associated with RV dyssynchrony by univariate and multivariate linear regression models

	Univariate		Multivariate (Model 1)		Multivariate (Model 2)	
	Correlation coefficient (95% CI)	P value	Correlation coefficient (95% CI)	P value	Correlation coefficient (95% CI)	P value
Clinical characteristics						
Body mass index (kg/m ²)	-0.136 (-0.292 to 0.026)	0.098				
Age (years)	-0.147 (-0.301 to 0.014)	0.074				
QRS duration (ms)	0.035 (-0.127 to 0.195)	0.676				
BNP (pg/mL)	0.078 (-0.085 to 0.237)	0.347				
Haemoglobin (mg/L)	0.037 (-0.125 to 0.197)	0.657				
Heart rate (b.p.m.)	0.224 (0.065-0.372)	0.006	0.160 (-0.021 to 0.341)	0.082	0.100 (-0.094 to 0.294)	0.310
Tricuspid regurgitation (0-4 grade)	-0.028 (-0.190 to 0.135)	0.736				
Haemodynamics						
PA mean pressure (mmHg)	0.168 (0.007-0.321)	0.041	0.157 (-1.265 to 1.580)	0.826	-0.088 (-1.453 to 1.630)	0.909
PA wedge pressure (mmHg)	0.163 (0.001-0.316)	0.048	-0.353 (-1.825 to 1.118)	0.635	-0.319 (-1.915 to 1.275)	0.693
Cardiac output (L/min)	-0.211 (-0.360 to -0.051)	0.010	-2.680 (-7.524 to 2.164)	0.276	-0.638 (-5.817 to 4.539)	0.807
Systolic blood pressure (mmHg)	0.009 (-0.153 to 0.169)	0.917				
Pulmonary vascular resistance (WU)	0.208 (0.047-0.358)	0.011	3.724 (-10.430 to 17.880)	0.603	3.330 (-12.010 to 18.672)	0.668
PA compliance (mL/mmHg)	-0.131 (-0.285 to 0.031)	0.114				
PA elastance (Ea) (mmHg/mL)	0.247 (0.089-0.392)	0.003				
RV systolic elastance (Ees) (mmHg/mL)	-0.272 (-0.415 to -0.116)	<0.001				
RV ventricular-arterial coupling ratio	-0.402 (-0.529 to -0.258)	<0.001	6.548 (-0.593 to 13.691)	0.072	-7.905 (-12.597 to -3.213)	0.001
RV diastolic compliance (mL/mmHg)	0.016 (-0.146 to 0.177)	0.847				
GSPECT						
RV end-diastolic volume (mL)	0.172 (0.011-0.325)	0.036				
RV end-systolic volume (mL)	0.353 (0.203-0.486)	<0.001				
RV ejection fraction (%)	-0.525 (-0.632 to -0.397)	<0.001	-0.800 (-1.148 to -0.486)	<0.001		
LV end-diastolic volume (mL)	0.182 (0.021-0.333)	0.027				
LV end-systolic volume (mL)	0.215 (0.055-0.364)	0.009				
LV ejection fraction (%)	-0.258 (-0.403 to -0.102)	0.002	-0.190 (-0.506 to 0.125)	0.234	-0.388 (-0.719 to -0.057)	0.022

BNP, brain natriuretic peptide; CI, confidence interval; GSPECT, gated single-photon emission computed tomography; LV, left ventricular; PA, pulmonary artery; RV, right ventricular; RVEF, right ventricular ejection fraction; WU, Wood units.

In the multivariable models, em dashes stand for variables not tested because of possible collinearity; meanwhile, empty rows mean that variables were not tested because of non-statistical significance in the univariate analysis. In multivariable Model 2, RVEF was excluded.

Figure 3 Change in (A) pulmonary artery (PA) wedge pressure, (B) right ventricular (RV) ejection fraction, and (C) RV dyssynchrony after sildenafil infusion ($N = 15$). Median values before and after sildenafil are reported on the relative sides of the chart. In (C), different colours represent changes in RV dyssynchrony tertiles of individual patients before and after sildenafil. Asterisk stands for $P < 0.05$.

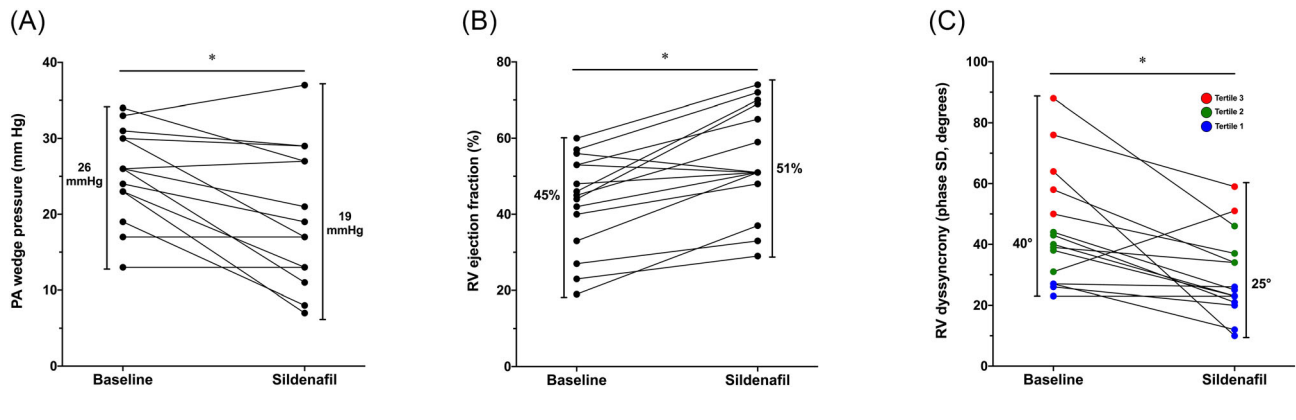
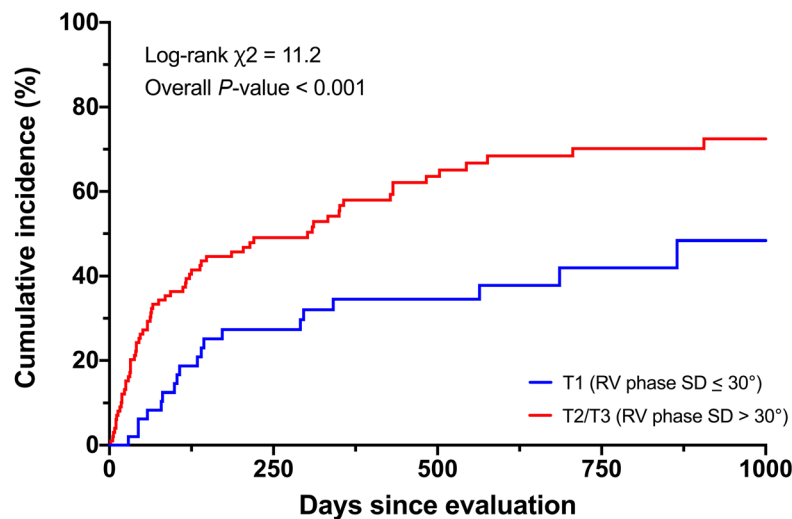


Figure 4 Kaplan–Meier curves for the composite outcome of death, urgent transplantation, or assist device implantation without heart transplantation stratified by right ventricular (RV) dyssynchrony tertiles.



No. at risk									
Tertile 1	49	39	32	26	22	19	11	9	7
Tertile 2/3	99	58	45	34	25	20	17	15	11

T1: hazard ratio [HR] 1.98 [95% confidence interval (CI) 1.20–3.24], $P = 0.007$. Even after adjusting Cox analysis for the variables independently associated with RV dyssynchrony at multivariable analysis (i.e. RVEF, LVEF, and right ventricular–arterial coupling), a higher degree of dyssynchrony remained associated with worse outcomes [T2/T3 vs. T1: HR 1.81 (95% CI 1.02–3.19), $P = 0.041$]. A sensitivity analysis using as primary endpoint the composite of death or urgent cardiac transplantation (i.e. excluding LVAD implantation, being this event possibly influenced by referral bias to our tertiary centre) showed similar results [T2/T3 vs. T1: HR 1.96 (95% CI 1.18–3.26), $P = 0.009$].

Discussion

Our findings show that among patients with advanced HFrEF and native ventricular conduction, increases in RV dyssynchrony correlated with impaired RV structure and function and were predictive of greater risk of adverse outcomes. Patients with more dyssynchronous RV shortening had greater impairments in ventricular chambers contractility by combined pressure–volume analysis and larger ventricular volumes. Higher RV dyssynchrony was associated with more adverse haemodynamics—such as increased RV afterload—and conversely, afterload reduction with sildenafil improved

RV synchrony. These data point to an important, previously unrecognized role for RV dyssynchrony as an adverse finding in HFrEF and suggest that therapies to improve RV synchrony, including RV afterload reduction, may be helpful to improve clinical outcomes in patients with advanced HFrEF.

Prior studies on RV dyssynchrony have focused almost exclusively on patients with PAH, where it constitutes an established and independent prognostic factor.^{2,29} In PAH, a combination of increased afterload and morphological RV remodelling was the major determinant of RV dyssynchrony.² As a novel observation, our study shows that the same parameters likely play a role in patients with HFrEF and RV dyssynchrony. Moreover, previous studies mainly focused on single imaging methods, meanwhile, our approach involved the simultaneous collection and combination of both dyssynchrony and pressure/volume data using GSPECT and RHC.

Increased afterload may induce RV dyssynchrony in HFrEF through several mechanisms. Due to the complex shape of the right ventricle, pulmonary hypertension causes inhomogeneity of RV's regional wall stress, leading to a non-uniform duration of contraction.^{30,31} Non-synchronous patterns of regional ventricular contraction impair overall RV systolic function, the strongest correlate of RV dyssynchrony in our study, meanwhile have less an impact on RV remodelling. Primary alterations of the LV³² or loading conditions³³ might further reduce the RV mechanical efficiency and consequently increase RV dyssynchrony in patients with HFrEF.³⁴ In this regard, previous experimental observations showed that LV contraction accounts for up to 40% of RV work, with septal contraction being the most important contributor to ventricular interdependence.³² In our study, we found that patients with LBBB had more RV dyssynchrony than patients with RBBB, regardless of QRS duration. This is not surprising, because LBBB induces a typically abnormal contraction of the interventricular septum with marked early systolic shortening and leftward motion,²⁴ reducing in turn RV systolic efficiency and intraventricular synchrony.⁴ On the contrary, RBBB-type delay shows modest effects on interventricular septum activation,³⁵ thus inducing a lower degree of dyssynchrony. Correcting LV dyssynchrony by CRT has been demonstrated to ameliorate RV dyssynchrony improving septum delay.⁴ In contrast to LV dyssynchrony, QRS duration was poorly correlated with RV dyssynchrony in HFrEF patients, as also demonstrated in previous studies among patients with PAH and in healthy volunteers.^{31,36}

Patients with non-ischaemic HF aetiology had a higher degree of RV dyssynchrony compared with patients with ischaemic HF. The most likely reason could be that the former group had a larger prevalence of primary myocardial tissue disease also affecting the right ventricle. In line, our finding that non-ischaemic HF patients showed larger RV volumes and lower RVEF compared with ischaemic patients seems to corroborate this hypothesis.

In our study, we observed a correlation between higher heart rate and the severity of RV dyssynchrony. Although causality cannot be clearly discerned from our data, it is worth to be noted that a higher heart rate might occur in sicker ventricles and/or in case of insufficient neurohormonal blockade, underlying the importance of the optimization of beta-blocker therapy in patients with HFrEF.

Increased afterload is also a major determinant of impaired RV systolic function. Indeed, afterload increase is the *primum movens* for the development of RV–PA uncoupling (i.e. the increase in RV contractility in response to increased afterload is not sufficient to support normal systolic function), leading in turn to a reduction in RV systolic (RVEF, RV Ees) and diastolic function, as well as to RV dilation,³⁷ all parameters strictly correlated with RV dyssynchrony in our study.

We show for the first time in patients with HFrEF that RV dyssynchrony can be acutely improved by afterload reduction. As previously demonstrated by our group, the acute infusion of a PDE5 inhibitor has RV afterload-reducing effects, decreasing PAWP predominantly through relief of pericardial restraint, and improves right ventricular–arterial coupling, RV volumes, and RVEF.^{38,39} This improved haemodynamic profile causes a relief in intraventricular systolic pressure, and consequently in wall stress in the basal segments, resulting in a reduction of dyssynchrony because of shortening of the time to the contraction onset in the RV free wall.⁴⁰ In agreement with our data, previous studies showed that acute hypoxia-induced raise in afterload induces a robust increase in RV dyssynchrony.^{33,36} These data support the importance of therapies to reduce PA pressures for improving RV shortening and synchrony in HFrEF. However, it should be emphasized that there is a lack of robust evidence from randomized clinical trials to substantiate the utilization of PAH-specific drugs in the management of pulmonary hypertension due to left heart disease in advanced and pre-transplant HFrEF patients.

We found only a marginal effect of preload modulation on RV dyssynchrony improvement. As cited above, elevated afterload can cause heterogeneity in RV regional wall stress, resulting in inhomogeneous duration of contraction.^{30,31} In particular, the time to reach peak contraction in the RV free wall is generally more delayed compared with the interventricular-septal wall.³¹ A recent healthy volunteers study showed that enhanced venous return may mitigate hypoxia-induced increases in RV dyssynchrony lengthening the time to peak contraction in the septum, aligning it with the RV free wall, and consequently reducing overall dyssynchrony.³³ The considerable duration of the leg rise manoeuvre (7 min) required for obtaining GSPECT volumetric data could potentially have caused significant volume redistribution, affecting to some extent the effect of preload increase on RV dyssynchrony. Differences in the studied populations and in the method of preload manipulation (lower body positive pressure vs. leg raise) may also account for the discrepancies between our study and previous literature. Interest-

ingly, we found that the effect of preload increases on RV dyssynchrony improvement became significant when tested in the subgroup of patients who underwent afterload reduction. This finding could be attributed to the higher RV afterload observed in the sildenafil group compared with the rest of the population, indicating a potentially enhanced role for preload modulation in this specific subset.

In our study, we showed that a higher degree of RV dyssynchrony was associated with worse outcomes, supporting clinical relevance of RV dyssynchrony in HFrEF patients. Although interesting, these findings should be interpreted in the context of the demonstrated strong associations between RV dyssynchrony, RV dysfunction, and RV afterload. RV pressure overload would cause RV dilatation and increased RV wall stress, leading to altered cell-to-cell electric coupling, non-uniform ventricular depolarization, and RV dyssynchrony. LBBB may further worsen the degree of RV dyssynchrony.³⁴

Limitations

The current study has inherent limitations. Patients were referred to our tertiary centre leading to selection bias. We did not study patients with mild HFrEF or patients with HF with preserved ejection fraction (HFpEF), so our findings cannot be extended to all spectra of HF. We report data on a sample consisting predominantly of males. However, we did not find any gender difference in RV dyssynchrony at baseline (data not shown), and previous observations failed to show any influence of sex on RV dyssynchrony response to alterations in preload and afterload.³³ RV Ees was determined using a simplified formula that did not take VO (theoretical volume of the unloaded ventricle) into account during the computation. Consequently, the accuracy of RV Ees estimation may have been influenced by the residual dependence of RV contractility on EDV, particularly when dealing with a dilated right ventricle. For the afterload reduction studies with sildenafil, each patient served as their own control, and there was no placebo arm, but this was not a clinical trial as sildenafil was administered as part of clinical practice to evaluate reversibility of pulmonary vascular disease in HFrEF. Some subjects in the control group showed borderline or mildly increased mPAP/PAWP. Similarly, controls showed, on average, an RV-PA coupling value at the lower limit of normality. These values were likely secondary to coexistent comorbidities such as hypertension, coronary artery disease, or mild pulmonary disease. Nevertheless, the differences in haemodynamics between the control and HFrEF group were wide and highly significant; in addition, all control subjects showed no relevant symptoms or signs of HF, ventricular dysfunction, or significantly elevated BNP levels. Therefore, it is likely that these findings had minimal impact on the validity of our control group. We conducted all measurements during spontaneous, uncon-

trolled breathing without breath-holding or respiratory gating, as we assumed that the respiration patterns were not significantly different between GSPECT and RHC. As a consequence, the combination of pressure and volume data might have increased data variability, compared with simultaneous approach. Preload increase was performed with a 7 min leg rise manoeuvre. A shorter passive leg raise, boosted with intravenous saline challenge, could have potentially resulted in more pronounced haemodynamic and dyssynchrony alterations. Owing to a technical limitation of the GSPECT machine, individuals with a heart rate exceeding 100 b.p.m. might experience a slight reduction in the accuracy of ventricular dyssynchrony evaluation. Likely due to the small sample size, we were able to show significant differences in the primary composite outcome only when categorizing the population based on a single threshold (e.g. PSD 30°). Nevertheless, this allowed us to define a subgroup with an increased risk of clinical events. It is theoretically possible that the decrease in LV afterload resulting from sildenafil administration could have potentially improved LV dyssynchrony and consequently participated to ameliorate RV dyssynchrony by reducing septum delay. Anyway, we cannot draw definite conclusions on this topic from current data. Furthermore, our study is primarily mechanistic, lacking direct or evident clinical implications. Finally, we cannot evaluate causality whether RV dyssynchrony is a cause or a consequence of RV dysfunction based upon the cross-sectional study design.

Conclusions

In this multimodality pressure-volume analysis in patients with advanced HFrEF, increased RV dyssynchrony was associated with higher RV afterload, lower contractility, and worse long-term outcome. Modulation of RV afterload attenuated the severity of RV mechanical dyssynchrony, identifying a possible therapeutic target. Further studies are warranted to determine whether amelioration of RV dyssynchrony by RV afterload reduction may help to improve RV performance in HFrEF.

Conflict of interest

None declared.

Funding

This work was supported by the Ministry of Health of the Czech Republic (Ministerstvo Zdravotnictví České Republiky), Agency for Healthcare Research (AZV), Grants NU22-02-

00161, NU21-02-00402, and NV19-02-00130, and by the project of the National Institute for Research of Metabolic and Cardiovascular Diseases (Program EXCELES, ID Project No. LX22NPO5104)—funded by the European Union—Next Generation EU. All rights reserved.

Supporting information

Additional supporting information may be found online in the Supporting Information section at the end of the article.

Table S1. Baseline characteristics of patients with HFrEF and controls.

Table S2. Imaging and hemodynamic data in patients with HFrEF and controls.

Table S3. Effect of afterload reduction (sildenafil) and preload increase (leg rise) on right ventricular dyssynchrony, hemodynamics and cardiac volumes derived from SPECT.

Figure S1. Three-dimensional reconstruction of ventricular end-diastolic (top row) and end-systolic (middle row) volumes and histograms of right ventricular (RV) phase standard deviation of systolic displacements (PSD) (bottom row) in controls and heart failure patients with low and high RV dyssynchrony. Abbreviations: Fwall, Right Ventricular Free Wall; Lat, Lateral Wall.

Figure S2. Bland–Altman plot for the intraoperator reproducibility of right ventricular (RV) A) end-diastolic volume (EDV) and B) end-systolic volume (ESV) measurements. The dashed line stands for the mean bias, the dotted lines represent the 95% limits of agreement.

Figure S3. Correlation between right ventricular (RV) dyssynchrony and A) pulmonary artery elastance; B) RV systolic elastance; C) right ventricular-arterial (RV-PA) coupling ratio; D) left ventricular (LV) end-diastolic volume; E) LV end-systolic volume; F) LV ejection fraction, all in HF patients.

Figure S4. Difference in A) right ventricular (RV) dyssynchrony; B) RV ejection fraction; C) RV end-diastolic volume and D) RV end-systolic volume among patient with ischemic and non-ischemic heart failure aetiology. Asterisk stands for $P < 0.05$.

Figure S5. Change in right ventricular (RV) dyssynchrony after leg rise (preload modulation) in the A) overall population ($N = 135$) and B) in the subgroup of patients underwent PDE5i administration to test afterload reduction ($N = 15$). Median values before and after sildenafil are reported on the relative sides of the chart. Different colours represent changes in RV dyssynchrony tertiles of individual patients before and after leg rise. Asterisk stands for $P < 0.05$.

Video S1. Control patient.

Video S2. Low RV dyssynchrony patient.

Video S3. High RV dyssynchrony patient.

References

- Bleeker GB, Bax JJ, Steendijk P, Schalij MJ, van der Wall EE. Left ventricular dyssynchrony in patients with heart failure: Pathophysiology, diagnosis and treatment. *Nat Clin Pract Cardiovasc Med* 2006;3:213-219. doi:10.1038/ncpcardio0505
- Badagliacca R, Reali M, Poscia R, Pezzuto B, Papa S, Mezzapesa M, *et al.* Right intraventricular dyssynchrony in idiopathic, heritable, and anorexigen-induced pulmonary arterial hypertension: Clinical impact and reversibility. *JACC Cardiovasc Imaging* 2015;8:642-652. doi:10.1016/j.jcmg.2015.02.009
- Tops LF, Prakasa K, Tandri H, Dalal D, Jain R, Dimaano VL, *et al.* Prevalence and pathophysiologic attributes of ventricular dyssynchrony in arrhythmogenic right ventricular dysplasia/cardiomyopathy. *J Am Coll Cardiol* 2009;54:445-451. doi:10.1016/j.jacc.2009.04.038
- Storsten P, Aalen JM, Boe E, Remme EW, Gjesdal O, Larsen CK, *et al.* Mechanical effects on right ventricular function from left bundle branch block and cardiac resynchronization therapy. *JACC Cardiovasc Imaging* 2020;13:1475-1484. doi:10.1016/j.jcmg.2019.11.016
- Fauchier L, Marie O, Casset-Senon D, Babuty D, Cosnay P, Fauchier JP. Interventricular and intraventricular dyssynchrony in idiopathic dilated cardiomyopathy: A prognostic study with Fourier phase analysis of radionuclide angioscintigraphy. *J Am Coll Cardiol* 2002;40:2022-2030. doi:10.1016/S0735-1097(02)02569-X
- Boogers MJ, Chen J, Veltman CE, van Bommel RJ, Mooyaart EA, Al Younis I, *et al.* Left ventricular diastolic dyssynchrony assessed with phase analysis of gated myocardial perfusion SPECT: A comparison with tissue Doppler imaging. *Eur J Nucl Med Mol Imaging* 2011;38:2031-2039. doi:10.1007/s00259-011-1870-5
- Rich JD, Ward RP. Right-ventricular function by nuclear cardiology. *Curr Opin Cardiol* 2010;25:445-450. doi:10.1097/HCO.0b013e32833cb252
- Fudim M, Fathallah M, Shaw LK, Liu PR, James O, Samad Z, *et al.* The prognostic value of diastolic and systolic mechanical left ventricular dyssynchrony among patients with coronary heart disease. *JACC Cardiovasc Imaging* 2019;12:1215-1226. doi:10.1016/j.jcmg.2018.05.018
- Singh H, Singhal A, Sharma P, Patel CD, Seth S, Malhotra A. Quantitative assessment of cardiac mechanical synchrony using equilibrium radionuclide angiography. *J Nucl Cardiol* 2013;20:415-425. doi:10.1007/s12350-013-9705-3
- Vallejo E, Jimenez L, Rodriguez G, Roffe F, Bialostozky D. Evaluation of ventricular synchrony with equilibrium radionuclide angiography: Assessment of variability and accuracy. *Arch Med Res* 2010;41:83-91. doi:10.1016/j.arcmed.2010.02.003
- Rosenkranz S, Preston IR. Right heart catheterisation: Best practice and pitfalls in pulmonary hypertension. *Eur Respir Rev* 2015;24:642-652. doi:10.1183/16000617.0062-2015
- Lavdaniti M. Invasive and non-invasive methods for cardiac output measurement. *Int J Caring Sci* 2008;1:6.
- Hesse B, Lindhardt TB, Acampa W, Anagnostopoulos C, Ballinger J, Bax JJ,

- et al. EANM/ESC guidelines for radionuclide imaging of cardiac function. *Eur J Nucl Med Mol Imaging* 2008;**35**:851-885. doi:10.1007/s00259-007-0694-9
14. Velleca A, Shullo MA, Dhital K, Azeka E, Colvin M, DePasquale E, et al. The International Society for Heart and Lung Transplantation (ISHLT) guidelines for the care of heart transplant recipients. *J Heart Lung Transplant* 2023;**42**:e1-e141. doi:10.1016/j.healun.2022.02.015
 15. Wright SP, Groves L, Vishram-Nielsen JKK, Karvasarski E, Valle FH, Alba AC, et al. Elevated pulmonary arterial elastance and right ventricular uncoupling are associated with greater mortality in advanced heart failure. *J Heart Lung Transplant* 2020;**39**:657-665. doi:10.1016/j.healun.2020.02.013
 16. Tello K, Richter MJ, Axmann J, Buhmann M, Seeger W, Naeije R, et al. More on single-beat estimation of right ventriculoarterial coupling in pulmonary arterial hypertension. *Am J Respir Crit Care Med* 2018;**198**:816-818. doi:10.1164/rccm.201802-0283LE
 17. Sanz J, Garcia-Alvarez A, Fernandez-Friera L, Nair A, Mirelis JG, Sawit ST, et al. Right ventriculo-arterial coupling in pulmonary hypertension: A magnetic resonance study. *Heart* 2012;**98**:238-243. doi:10.1136/heartjnl-2011-300462
 18. Vonk Noordegraaf A, Chin KM, Haddad F, Hassoun PM, Hemnes AR, Hopkins SR, et al. Pathophysiology of the right ventricle and of the pulmonary circulation in pulmonary hypertension: An update. *Eur Respir J* 2019 Jan;**53**:1801900. doi:10.1183/13993003.01900-2018
 19. Tello K, Dalmer A, Axmann J, Vanderpool R, Ghofrani HA, Naeije R, et al. Reserve of right ventricular-arterial coupling in the setting of chronic overload. *Circ Heart Fail* 2019;**12**:e005512. doi:10.1161/CIRC. HEARTFAILURE.118.005512
 20. Simonneau G, Montani D, Celermajer DS, Denton CP, Gatzoulis MA, Krowka M, et al. Haemodynamic definitions and updated clinical classification of pulmonary hypertension. *Eur Respir J* 2019;**53**:1801913. doi:10.1183/13993003.01913-2018
 21. Fudim M, Dalgaard F, Fathallah M, Iskandrian AE, Borges-Neto S. Mechanical dyssynchrony: How do we measure it, what it means, and what we can do about it. *J Nucl Cardiol* 2021;**28**:2174-2184. doi:10.1007/s12350-019-01758-0
 22. Friehling M, Chen J, Saba S, Bazaz R, Schwartzman D, Adelstein EC, et al. A prospective pilot study to evaluate the relationship between acute change in left ventricular synchrony after cardiac resynchronization therapy and patient outcome using a single-injection gated SPECT protocol. *Circ Cardiovasc Imaging* 2011;**4**:532-539. doi:10.1161/CIRC. IMAGING.111.965459
 23. Chen J, Garcia EV, Folks RD, Cooke CD, Faber TL, Tauxe EL, et al. Onset of left ventricular mechanical contraction as determined by phase analysis of ECG-gated myocardial perfusion SPECT imaging: Development of a diagnostic tool for assessment of cardiac mechanical dyssynchrony. *J Nucl Cardiol* 2005;**12**:687-695. doi:10.1016/j.nuclcard.2005.06.088
 24. Van Kriekinge SD, Nishina H, Ohba M, Berman DS, Germano G. Automatic global and regional phase analysis from gated myocardial perfusion SPECT imaging: Application to the characterization of ventricular contraction in patients with left bundle branch block. *J Nucl Med* 2008;**49**:1790-1797. doi:10.2967/jnumed.108.055160
 25. Trimble MA, Velazquez EJ, Adams GL, Honeycutt EF, Pagnanelli RA, Barnhart HX, et al. Repeatability and reproducibility of phase analysis of gated single-photon emission computed tomography myocardial perfusion imaging used to quantify cardiac dyssynchrony. *Nucl Med Commun* 2008;**29**:374-381. doi:10.1097/MNM.0b013e3282f81380
 26. Melenovsky V, Kotrc M, Borlaug BA, Marek T, Kovar J, Malek I, et al. Relationships between right ventricular function, body composition, and prognosis in advanced heart failure. *J Am Coll Cardiol* 2013;**62**:1660-1670.
 27. Monzo L, Kotrc M, Benes J, Sedlacek K, Jurcova I, Franekova J, et al. Clinical and humoral determinants of congestion in heart failure: Potential role of adiponectin. *Kidney Blood Press Res* 2019;**44**:1271-1284. doi:10.1159/000502975
 28. Aaronson KD, Schwartz JS, Chen TM, Wong KL, Goin JE, Mancini DM. Development and prospective validation of a clinical index to predict survival in ambulatory patients referred for cardiac transplant evaluation. *Circulation* 1997;**95**:2660-2667. doi:10.1161/01. CIR.95.12.2660
 29. Murata M, Tsugu T, Kawakami T, Kataoka M, Minakata Y, Endo J, et al. Right ventricular dyssynchrony predicts clinical outcomes in patients with pulmonary hypertension. *Int J Cardiol* 2017;**1**:912-918. doi:10.1016/j.ijcard.2016.11.244
 30. Calcutteea A, Chung R, Lindqvist P, Hodson M, Henein MY. Differential right ventricular regional function and the effect of pulmonary hypertension: Three-dimensional echo study. *Heart* 2011;**97**:1004-1011. doi:10.1136/hrt.2010.208900
 31. Marcus JT, Gan CT, Zwanenburg JJ, Boonstra A, Allaart CP, Gotte MJ, et al. Interventricular mechanical asynchrony in pulmonary arterial hypertension: Left-to-right delay in peak shortening is related to right ventricular overload and left ventricular underfilling. *J Am Coll Cardiol* 2008;**51**:750-757. doi:10.1016/j.jacc.2007.10.041
 32. Buckberg G, Hoffman JI. Right ventricular architecture responsible for mechanical performance: Unifying role of ventricular septum. *J Thorac Cardiovasc Surg* 2014;**148**:3166-3171. doi:10.1016/j.jtcvs.2014.05.044
 33. Ewalts M, Dawkins T, Boulet LM, Thijssen D, Stembridge M. The influence of increased venous return on right ventricular dyssynchrony during acute and sustained hypoxaemia. *Exp Physiol* 2021;**106**:925-937. doi:10.1113/EP088657
 34. Mashali MA, Saad NS, Peczkowski KK, Fanning T, Hare AN, Whitson BA, et al. Mechanical dyssynchrony of isolated left and right ventricular human myocardium in end-stage heart failure. *Circ Heart Fail* 2023;e009871. doi:10.1161/CIRCHEARTFAILURE.122.009871
 35. Byrne MJ, Helm RH, Daya S, Osman NF, Halperin HR, Berger RD, et al. Diminished left ventricular dyssynchrony and impact of resynchronization in failing hearts with right versus left bundle branch block. *J Am Coll Cardiol* 2007;**50**:1484-1490. doi:10.1016/j.jacc.2007.07.011
 36. Pezzuto B, Forton K, Badagliacca R, Motoji Y, Faoro V, Naeije R. Right ventricular dyssynchrony during hypoxic breathing but not during exercise in healthy subjects: A speckle tracking echocardiography study. *Exp Physiol* 2018;**103**:1338-1346. doi:10.1113/EP087027
 37. Vonk Noordegraaf A, Westerhof BE, Westerhof N. The relationship between the right ventricle and its load in pulmonary hypertension. *J Am Coll Cardiol* 2017;**69**:236-243. doi:10.1016/j.jacc.2016.10.047
 38. Monzo L, Reichenbach A, Al-Hiti H, Borlaug BA, Havlenova T, Solar N, et al. Active unloading effects of sildenafil enhance right ventricular-pulmonary artery coupling in heart failure. *J Card Fail* 2021;**27**:224-232. doi:10.1016/j.cardfail.2020.11.007
 39. Monzo L, Reichenbach A, Al-Hiti H, Jurcova I, Huskova Z, Kautzner J, et al. Pulmonary vasculature responsiveness to phosphodiesterase-5A inhibition in heart failure with reduced ejection fraction: Possible role of plasma potassium. *Front Cardiovasc Med* 2022;**9**:883911. doi:10.3389/fcvm.2022.883911
 40. Palau-Caballero G, Walmsley J, Van Empel V, Lumens J, Delhaas T. Why septal motion is a marker of right ventricular failure in pulmonary arterial hypertension: Mechanistic analysis using a computer model. *Am J Physiol Heart Circ Physiol* 2017;**312**:H691-H700. doi:10.1152/ajpheart.00596.2016